Journal of
Renewable Energy Research and Applications (RERA)

Vol. 4, No. 2, 2023, 251-258 DOI: 10.22044/rera.2023.12555.1192

Assessment of Rooftop Solar Power Potential in Rural Areas using UAV Photogrammetry and GIS

A. Baghani

Department of Surveying Engineering, Golestan University, Aliabad Katul, Iran.

Received Date 26 December 2022; Revised Date 29 January 2023; Accepted Date 08 February 2023
**Corresponding author: a.baghani@gu.ac.ir (A. Baghani)*

Abstract
In the recent years, the growing demand for energy and environmental requirements has focused much attention on the solar energy as a renewable source. The building rooftops are the most suitable places for installing photovoltaic panels in the urban and rural areas. In large districts, accurate estimation of radiation received by the rooftops requires the existence of detailed 3D information about them. This research work aims to provide an efficient method to estimate the solar energy production potential from the rooftops using the UAV photogrammetry method and GIS. The proposed method considers both the factors of the geometric features of the rooftops (slope and azimuth) and the shadow of the adjacent features. A threshold for minimum separated suitable rooftops for installing photovoltaic panels received radiation and rooftop area. Converting the received radiation into electrical energy was made based on the average level of current world technology for solar panels. Providing a comparison between the amount of electricity produced during the four seasons and throughout the year as an effective parameter related to the consumption pattern is another achievement of this research work. The findings of this work can be used in various fields such as electricity and the construction industry, as well as macro-planning, to benefit from clean energy. The results of implementing the proposed method for a rural area show that out of a total of 543 existing roofs, 422 roofs are suitable for installing solar panels. Also for these rooftops, the potential to produce 5741 MWh of electricity will be available in one year.

Keywords: *Renewable Energy, Photovoltaic, Photogrammetry, Geographic Information System, Digital Elevation Model.*

1. Introduction

The utilization of renewable energies has faced significant growth in the recent years, so we are witnessing severe investments by governments for their utilization. The development of solar energy extraction technologies is evident in both countries rich in hydrocarbon resources (such as the Persian Gulf countries) and countries that do not benefit from solar radiation (such as European countries) [1]. For example, in the center of Europe in 2020, Germany provided only 48,641 GWh of its electricity needs through solar energy. This value is 10953 GWh for Turkey [2]. It is also worth mentioning that Saudi Arabia has targeted solar electricity production of about 350,000 GWh by 2030 [1].

Despite being on the belt with the most solar radiation, Iran has produced only 584 GWh of its energy needs from this source [3]. The significant advantages of using solar radiation, compared to other sources, explain the necessity of planning to benefit from this energy source. Photovoltaic systems can be implemented more effectively and cheaply by individuals or governments in small or large areas than other energy sources [4]. One of the essential advantages of using photovoltaic systems is their availability, relatively low cost, and the possibility of independently implementing them for residential units. Considering its geographical location and weather conditions, Iran has a high potential for using solar energy. On the other hand, the growing population and the increasing industrial needs of the country, along with the air pollution caused by the consumption of fossil fuels, reinforce the need to use solar power as a clean source.

Due to the dependence of the received radiation of each point on the earth's surface on spatial information, a large part of the research works in this field aimed at estimating the potential of using photovoltaic systems to generate electricity based on the spatial data [5]. Assessing the potential of rooftop solar energy has taken a significant part of the research. Various methods have been developed for this purpose; most of them have used GIS tools to calculate the amount of energy received using the data of the Digital Surface Model (DSM) [6]. Three data sources including lidar, CAD-based model, and recently, the UAV photogrammetry method, have also been mainly used as a basis for DSM production [7]. Due to its high cost and less accessibility, aerial lidar has not been very popular among the methods of evaluating the potential of solar energy. In addition, the relatively low density of point cloud obtained from lidar compared to the UAV photogrammetry method may make it difficult to get a high-detail DSM on the rooftops, and consequently, to estimate the amount of received radiation accurately.

Using a CAD-based model instead of the realistic 3-D model for rooftops, the radiation received by the rooftops can not be assessed correctly. The effect of shadows will be omitted, and the impact of geometrical parameters of the rooftop (slope and azimuth) will be neglected in radiation computation. Some existing methods are also based on the mapping of 2D outlines on elevation models. Due to their low of level of details, they cannot provide a complete geometrical description of the rooftops. As a result, an accurate estimate of the energy production potential cannot be estimated based on 2D CAD-based maps [8].

Also a large part of the research is devoted to evaluating the potential of receiving solar energy on the earth's surface. A lesser part is devoted to estimating the amount of radiation received and the electricity produced from the rooftops, especially using accurate and detailed 3D models. A general evaluation of the potential of receiving solar radiation in the country of Eritrea was carried out in research [9].

The UAV photogrammetry method has many applications, especially in the field of spatial information. Mapping [10], forestry [11], archeology [12], natural hazard studies [13], geology [14], etc. are among these applications. However, there are a few research works regarding solar energy potential studies using the UAV photogrammetry method.

In this research work, rooftops are not investigated for photovoltaic panel installation; just an overall estimate of solar radiation is calculated. Meanwhile, installing solar panels on the roofs of buildings in urban and rural areas has many advantages over other surfaces. Among these advantages are the amount of receiving more energy with less influence from shadows and disturbing effects, less vulnerability with more extended durability, and no need for a transmission network and related equipment to direct the flow of produced electricity to consumption sources [15].

By studying the previous research works, we can see that various data have been used to calculate the received radiation, which is mainly suitable for general studies. Due to their low resolution and level of detail, they are inefficient for studies requiring high accuracy. On the other hand, checking the suitability of roofs for installing photovoltaic panels and the possibility of calculating the amount of electricity produced for each rooftop separately and in each predetermined historical period are among other things that have not been investigated in previous research [16]. Also most of these research works have only calculated the amount of received radiation, and have not examined the amount of electricity that can be extracted. Another thing that has not been addressed is the need to accurately assess the potential of solar energy during different seasons of the year according to the amount of energy required in each season.

This study investigated the potential of rooftops for solar energy production using GIS as a computing tool and UAV photogrammetry as the method for generating the base data. Due to some limitations and problems arising from the DSM/DTM used in rooftop solar power potential estimation, in this study, the UAV photogrammetry method was used to produce the DSM of the studied area. Using GIS tools and rooftops extracted from DSM, each rooftop's exact amount of received radiation was calculated separately. The roofs lacking the necessary qualification for solar panel installation were identified, and the received radiation was converted into electricity for suitable rooftops. The proposed method was implemented in a rural area in the north of Iran. For the four seasons and throughout the year, rooftop solar power potential was assessed, and the results were analyzed.

2. Materials and methods

The flowchart presented in figure 1 shows the basic steps of the proposed method. The detailed steps and the implementation and evaluation of its results are presented in the following.

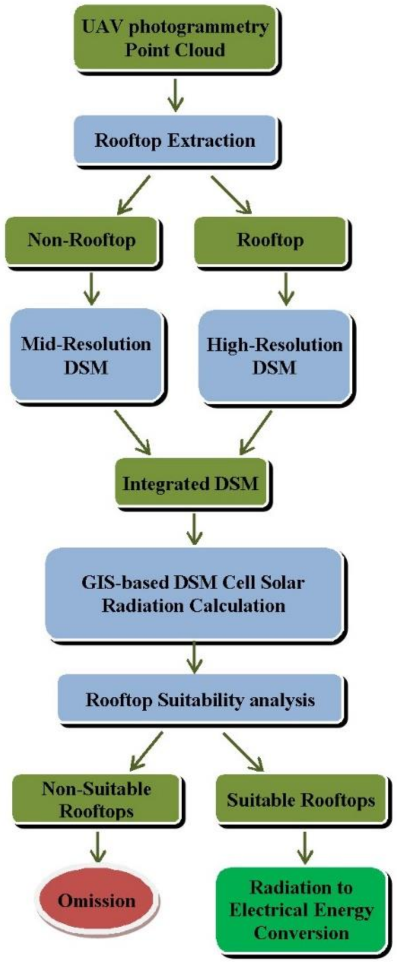

Figure 1. Structural framework of this study.

2.1. Studied area

Gol-Ceshmeh village, located in the central areas of Golestan province-Iran, with an approximate height of 60 m above the mean sea level and an approximate area of 40 hectares, was selected as the studied area. This village has a relatively large number of trees and buildings with sloping and flat roofs. Figure 2 shows the geographical location of the studied area on the annual solar radiation map of Iran.

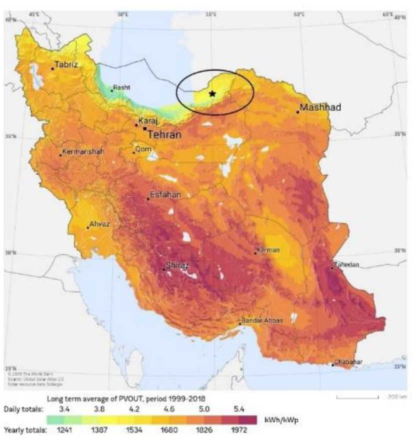

Figure 2. Geographical location of studied area [17].

The orthophoto and DSM, which contain information about the study area, are presented in figure 3.

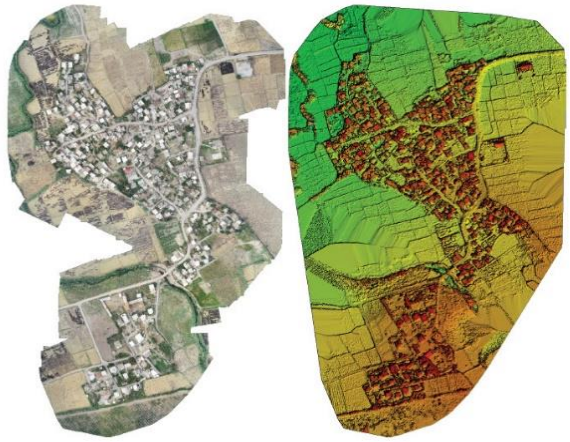

Figure 3. Orthophoto and DSM of studied area.

2.2. DSM generation using UAV photogrammetry

Calculating the exact amount of received radiation for each point requires having accurate spatial information about that point and its surroundings. For each point, the relative position of the sun and the time of radiation are among the most important influencing factors. Regarding the rooftops, the two geometric features of slope and azimuth are of great importance in the amount of radiation received [18]. Due to estimating the amount of radiation received by each cell of DSM, the result is sensitive to its resolution and level of detail.

This study used the point cloud obtained from the UAV photogrammetry method to produce DSM. Aerial imaging of the studied area was done in a convergent network with 80% forward and 60% lateral overlap. Georeferencing was made in the WGS84-coordinate system and UTM-map projection using 15 ground control points with proper distribution in the studied area. The Agisoft PhotoScan 1.2.6 software [19], based on the dense matching algorithm, was used to generate the point cloud. The point cloud density was estimated at an average of 97 points per square meter. The photogrammetric accuracy assessment of the point cloud showed an average of 3 cm and 5 cm of planimetric and altimetric accuracy.

Figure 4 shows a part of the 3D model produced for the studied area. As it can be seen from this figure, the features (especially the roofs) in the 3D model have a high level of detail. As a result, it is possible to calculate the radiation received by any point on the rooftop concerning shadow and geometric effects.

Figure 4. A representation of the dense point cloud used to generate DSM.

In the presence of noises, the extraction of geometric parameters such as slope from DSM can be accompanied by significant errors; in this study, a low-pass filter was used for noise reduction of rooftops point cloud; for this purpose, the method presented in [20] was used. In each neighborhood with a number of 10 points, the distances of the neighboring points to the center of the neighborhood were calculated, and the points with a distance greater than the average distance plus one time the standard deviation of the distances were removed.
Due to the importance of building rooftops in DSM data than other features, a two-scale strategy was used in generating DSM from the point cloud, corresponding to two levels of features including roof and non-roof. In this way, the roofs requiring a high level of detail were structured with more resolution than non-roof areas. For this purpose, the DSM cells were grouped into two parts, located on the roof and non-located. The cells inside the roofs were structured with 10 cm, and other cells with 40 cm resolution. The final model was created by combining two DSMs with different resolutions related to roof and non-roof. Due to the high resolution of the produced DSM, it will be possible to calculate the potential of solar energy because of the geometrical specification of rooftops and applying the shadow effects caused by adjacent features to the building roofs.

2.3. Rooftop solar radiation assessment

Solar radiation received by different surfaces consists of two parts: direct radiation (RadDir) and diffuse radiation (RadDif) [21]. Direct radiation, which includes most of the energy, results from direct sunlight hits on surfaces. The radiation scattered by the atmosphere or the surrounding objects that hit surfaces in a scattered form is also known as diffuse radiation. The diffused radiation is lower than direct radiation, and its calculation is not as easy as direct radiation. Equation 1 shows the mathematical model used to calculate the amount of received radiation [22].

$$\mathbf{Rad_{Glob} = Rad_{Dir} + Rad_{Dif}} \quad (1)$$

In this study, the amount of radiation received by each DSM cell is calculated based on two datasets, DSM and the rooftop outlines of buildings. In the first step o radiation calculation, using the solar radiation tool in the ArcGIS Pro software, the amount of received radiation was calculated for each DSM cell. The scatter rate and transmittance coefficient values were set to 0.3 and 0.5, respectively. The sky size was considered 100 m, and the daily time interval was also set to 1 hour. Calculations related to the amount of received radiation in time in two situations: throughout one solar year and the four seasons were done separately.
In the next step, using the roof layer of the buildings, the amount of radiation received for each rooftop was separated from the generated global radiation data. Finally, each roof's radiation was calculated separately using the cells inside that roof. Figure 5 shows the calculated received radiation for all DSM cells of the studied area for spring, summer, autumn, and winter.
Figure 6 shows the received radiation results only for the roof cells. The amount of radiation received throughout the year for all DSM cells and only rooftop cells are presented separately in figure 7.

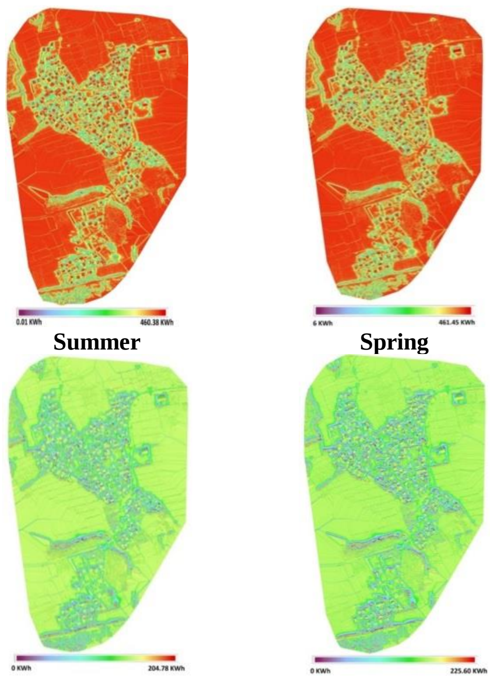

Figure 5. A representation of radiation received by studied area in different seasons of the year.

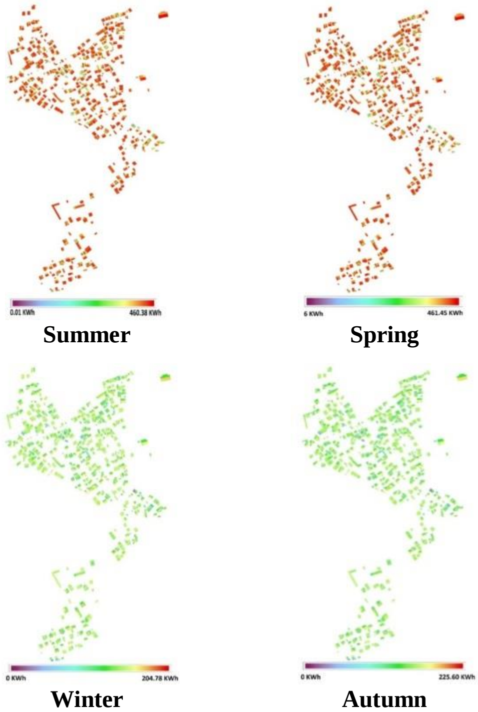

Figure 6. A presentation of the received radiation of the roofs of the studied area in different seasons of the year.

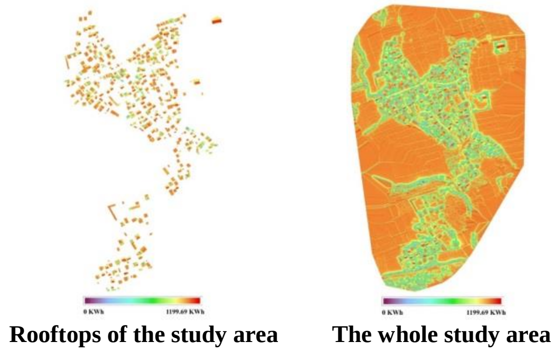

Figure 7. A presentation of annual received radiation.

The results presented in figures 5, 6, and 7 are in KWh in the period specified for each figure. The numerical values of the average radiation received per square meter from the roofs of the study area for the four seasons are given separately in table 1. As can be seen from figures 5 to 7 and table 1, The amount of radiation received in the summer and spring is similar. Also, the autumn and winter seasons are similar in this respect. The amount of solar radiation in the first two months is almost twice as much as in the second two months of the year.

Table 1. Amount of radiation received by the rooftops in kWh and kWh/m2

Season	Spring	Summer	Automn	Winter
The total radiation received by the rooftops (KWh)	14848.75	14792.14	5304.54	4946.42
The average radiation received by the rooftops (kWh/h2)	395.47	393.97	140.19	130.74

The amount of radiation received for all rooftops throughout the year was estimated to be 40248.05 MWh, and its average for each square meter of rooftops during a year was estimated to be 1194.70 KWh/m^2. Figure 8 shows the statistical distribution of the average radiation received by the roofs for each square meter.

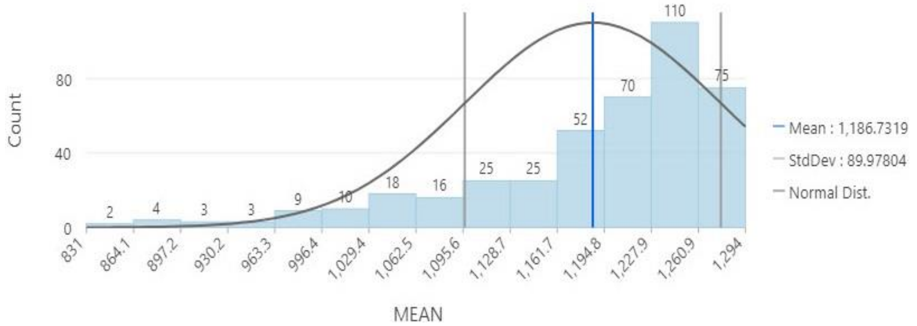

Figure 8. Statistical distribution of the average amount of radiation received per square meter of rooftops.

The values listed in Figure 8 show the radiation each roof receives throughout the year. The difference in the received radiation values is mainly caused by the area of each roof and its slope and azimuth. Figure 9 shows the results of estimating the amount of annual radiation received for some rooftops. This figure shows that the rooftops oriented towards the south have received the most radiation.

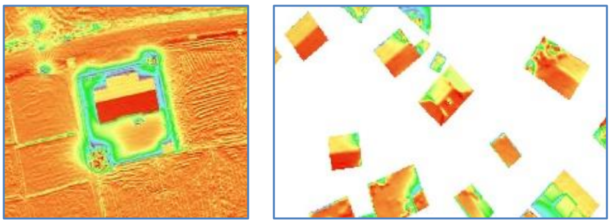

Figure 9. A presentation of the effect of azimuth, slope, and area on rooftop radiation.

2.4. Converting rooftop solar radiation into electricity

The values listed in table 1 indicate the amount of energy that can be received by the entire surface of each roof. Not all rooftops can be completely covered by solar panels, and not all the energy received can be converted into electricity. On the other hand, some roofs do not receive enough radiation due to improper slope and azimuth. Temperature and atmospheric conditions, along with the efficiency rate of the solar panel, are among the other determining factors in the conversion factor of received radiation into electricity.

In order to achieve a realistic estimate of the amount of electricity produced by solar panels installed on the rooftops, two stages of refinement were applied by thresholding the roof's minimum area and the minimum received radiation. Following the suitable rooftop selection step, conversion of the received radiation into electricity was performed by considering solar panel efficiency and the maximum coverable area of the rooftop.

In the first refinement step, rooftops with an area of less than 30 m^2 were removed from the set of rooftops. In the second step, roofs with an average received radiation less than a calculation threshold were excluded from the suitable rooftops.

In order to calculate the threshold of the minimum received radiation, the mean received radiation of the rooftops (Rad_{Glob}^{Mean}) was calculated, and the rooftops whose received radiation is less than $0.33{*}Rad_{Glob}^{Mean}$ were labeled as non-suitable rooftops.

The total number of rooftops in the studied area was 543, and according to the refinement step, 422 rooftops were selected as suitable rooftops. In figure 10, rooftops distinguished from others with a highlight color are identified as eligible for solar panel installation based on the rooftop solar radiation refinement step.

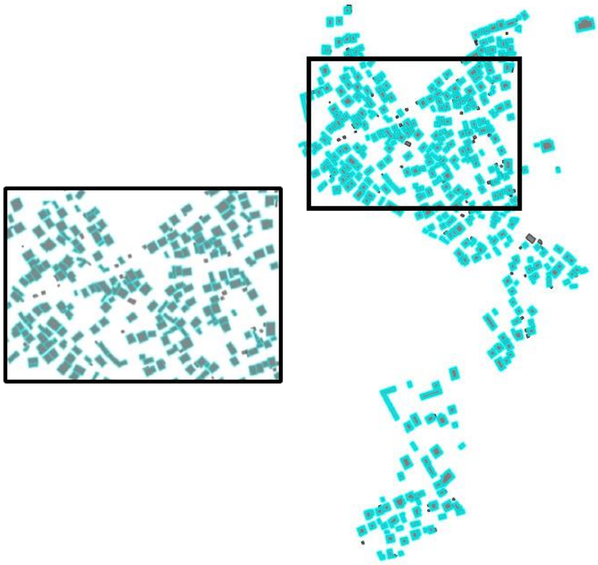

Figure 10. A presentation of the suitable rooftop detection results.

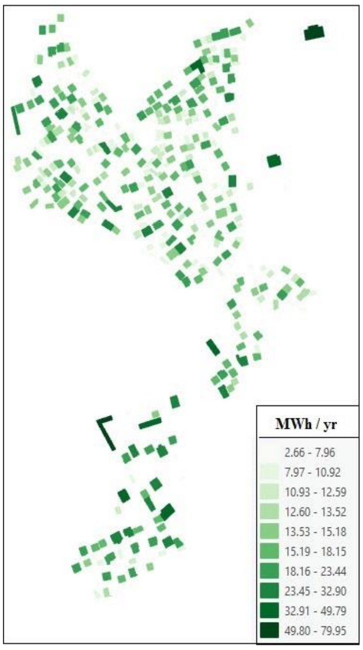

Figure 11. A presentation of the distribution of electricity produced by suitable rooftops in MWh/yr.

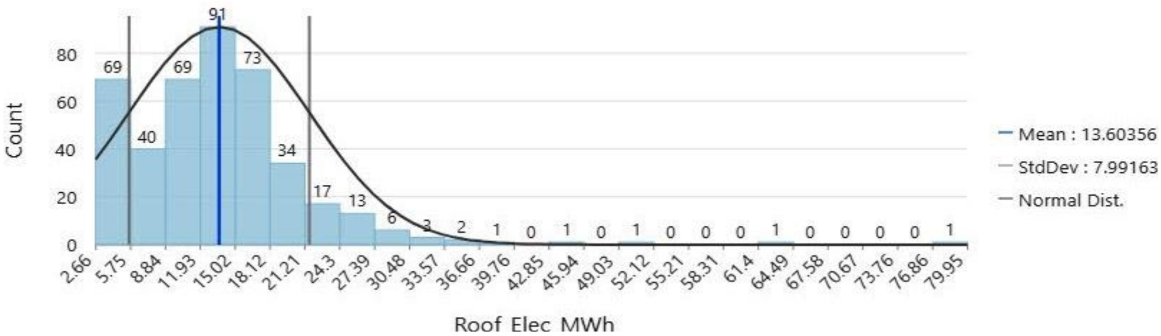

Figure 12. Statistical distribution of the amount of energy produced by each rooftop.

This study calculated the amount of electricity produced from the rooftops for only the roofs identified as suitable for installing solar panels. In order to convert the received radiation into electrical energy, the standard introduced by the United States Environmental Protection Agency [23] was used (Equation 2). This standard considers a conservative estimate for converting the amount of radiation received into electricity including an efficiency factor of 16% and a performance ratio of 86%. These numbers mean that solar panels, according to the world's average technology, can convert 16% of the received radiation into energy and then convert 86% of this energy into electricity for use by consumption sources. Rad_{Glob} stands for the amount of solar radiation received during a year in terms of MWh, and $Elec_{Glob}$ stands for the amount of electricity produced equivalent to it in terms of MWh.

$$\mathbf{Elec_{Glob} = Rad_{Glob}*0.16*0.86} \quad (2)$$

The amount of electrical energy produced from suitable rooftops, according to equation 2, was estimated at 5741 MWh/yr. This amount has been estimated for 422 suitable rooftops out of 543 rooftops in the studied area. The maximum annual electricity production is 80 MWh, which corresponds to the roof with the largest area (459 m^2). Also the result of converting the received radiation to electrical energy is noticeable in figure 11. The distribution diagram of the amount of energy produced by each of the rooftops is also presented in figure 12. Based on the results presented in this figure, most of the rooftops of the studied area can produce electrical energy in the range of 6 MWh to 23 MWh. Also 15 MWh of electricity are the most abundant in the amounts of energy produced by each rooftop. According to figures 11 and 12, roofs with a larger area protected from the shadow of other effects such as trees or nearby buildings will have a higher chance of receiving solar radiation. Also the impact of two geometrical specifications of the rooftops, slope, and azimuth, is evident in the results of receiving energy and producing electricity by roofs. The south-oriented roofs with slopes between 30 and 50 degrees receive the most radiation. Figure 9 can explain this issue well. Therefore, installing panels along the optimal slopes can increase the amount of electricity extracted.

3. Conclusion

This work addressed the issue of estimating the rooftop solar power potential based on UAV photogrammetry and GIS. Due to the high importance of the DSM in estimating rooftop solar radiation, the photogrammetric high-resolution point cloud was used as the basis for the DSM creation. First, the proposed method extracted the rooftops from the photogrammetric point cloud with a high level of detail. Then the amount of radiation received by the roofs was estimated in four seasons and throughout the year using GIS. The subsequent refinement step was designed to identify suitable rooftops for covering by photovoltaic panels. Therefore, suitable roofs entered the step of converting the received radiation into electricity in the next step. A flexible mathematical model was adopted for this purpose, which is compatible with the average solar panels' efficiency and a standard coverable area of the rooftop.

The proposed method was implemented for different seasons and throughout the year. The results show an increase of about two times the amount of solar energy in spring and summer compared to autumn and winter. Also the potential of solar energy that could be extracted for two seasons, spring and summer, and two seasons, autumn and winter, showed relative values. The results of implementing the proposed method for a rural area in the Golestan province of Iran showed that out of the 543 rooftops, 422 were suitable for installing photovoltaic panels. For suitable rooftops, the potential to produce 4600 MWh of electricity in one year was estimated, which can lead to the village's self-sufficiency from other energy sources. The results indicate the effect of two important geometric features of roofs: azimuth and slope, on the amount of radiation received by them. These two parameters can be considered the essential factors in installing photovoltaic panels. Their optimal setting can increase the amount of produced solar energy compared to the estimated values in this study. The high flexibility of the proposed method in calculating the production energy potential by using various strategies is one of the other advantages of the method presented in this research.

4. References

[1] Alhammad, A., Sun, Q., and Tao, Y. (2022). Optimal Solar Plant Site Identification Using GIS and Remote Sensing: Framework and Case Study. Energies, 15, 312. https://doi.org/10.3390/en15010312.

[2] Teofilo, A., Radosevic, N., Tao, Y., Iringan, J., and Liu, C. (2021) Investigating potential rooftop solar energy generated by Leased Federal Airports in

Australia: Framework and implications. J. Build. Eng, 41, 102390.

[3] Momenzadeh, Z., kalantari, S., Tazeh, M., and Taghizadeh, R. (2021). 'Zoning and locating solar power station using AHP and GIS in Yazd province', Journal of Environmental Science and Technology, 22(12), pp. 259-271. doi: 10.22034/jest.2020.37606.4373.

[4] Lukač, N., Seme, S., Žlaus, D., Štumberger, G., and Žalik, B., (2014). Buildings roofs photovoltaic potential assessment based on LiDAR (Light Detection And Ranging) data, energy, 66, PP. 598-609.

[5] Colak, H. E., Memisoglu, T., and Gercek, Y. (2020). Optimal site selection for solar photovoltaic (PV) power plants using GIS and AHP: a case study of Malatya Province, Turkey, Renew. Energy, 149, pp. 565-576, 10.1016/j.renene.2019.12.078.

[6] Holmberg, K. and Erdemir, A. (2017). Influence of tribology on global energy consumption, costs and emissions. Friction, 5, 263–284.

[7] HOFIERKA, J.; ZLOCHA, M. (2012). A New 3-D Solar Radiation Model for 3-D City Models. Transactions in GIS, 16 (5), 681-690.

[8] Doljak, D. *et al*. (2017). Photovoltaic Potential of the City of Pozarevac, Renewable and Sustainable Energy Reviews, 73, June, pp. 460-467.

[9] Ghebrezgabher, M. and Weldegabir, A. (2022). 'Estimating Solar Energy Potential in Eritrea: a GIS-based Approach', Renewable Energy Research and Applications, 3(2), pp. 155-164. doi: 10.22044/rera.2022.11737.1106.

[10] Nex, F. and Remondino, F. UAV for 3D mapping applications: A review. Appl. Geomat. 2014, 6, 1–15.

[11] Iglhaut, J.; Cabo, C.; Puliti, S.; Piermattei, L.; O'Connor, J.; and Rosette, J. Structure from motion photogrammetry in forestry: A review. Curr. For. Rep. 2019, 5, 155–168.

[12] Gasparini, M.; Moreno-Escribano, J.C.; and Monterroso-Checa, A. Photogrammetric Acquisitions in Diverse Archaeological Contexts Using Drones: Background of the Ager Mellariensis Project (North of Córdoba-Spain). Drones 2020, 4, 47.

[13] Kucharczyk, M. and Hugenholtz, C. H. (2021). Remote sensing of natural hazard-related disasters with small drones: Global trends, biases, and research opportunities. Remote Sensing of Environment, 264, 112577.

[14] Vasuki, Y., Holden, E., Kovesi, P., and Micklethwaite, S. (2014). Semi-automatic mapping of geological Structures using UAV-based photogrammetric data: An image analysis approach. Computers & Geosciences, 69, 22-32.

[15] Schunder, T., Yin, D.; Bagchi-Sen, S., and Rajan, K. (2020). A Spatial Analysis of the Development Potential of Rooftop and Community Solar Energy. Remote Sens. Appl. Soc. Environ., 19, 100355.

[16] Huang, X., Hayashi, K., Matsumoto, T., Tao, L., Huang, Y., and Tomino, Y. (2022). Estimation of Rooftop Solar Power Potential by Comparing Solar Radiation Data and Remote Sensing Data—A Case Study in Aichi, Japan. Remote Sens, 14, 1742. https://doi.org/10.3390/rs14071742.

[17] http://globalsolaratlas.info (Accessed: 10 November 2022).

[18] Esfahani, S. K., Karrech, A., Cameron, R., Elchalakani, M., Tenorio, R., and Jerez, F. (2021). Optimizing the solar energy capture of residential roof design in the southern hemisphere through Evolutionary Algorithm. Energy and Built Environment, 2(4), 406-424.

[19] https://www.agisoft.com/ (Accessed: 12 November 2022).

[20] Baghani, A., Valadan Zoej, M. J., and Mokhtarzade, M (2018) Automatic hierarchical registration of aerial and terrestrial image-based point clouds, European Journal of Remote Sensing, 51:1, 436-456,
DOI: 10.1080/22797254.2018.1444946.

[21] Avtar, R.; Sahu, N., Aggarwal, A.K., Chakraborty, S., Kharrazi, A., Yunus, A.P., Dou, J.; and Kurniawan, T.A. (2019). Exploring Renewable Energy Resources Using Remote Sensing and GIS—a Review. Resources, 8, 149.

[22] Phap, V.M., Thu Huong, N.T., Hanh, P.T., Van Duy, P., and Van Binh, D. (2020). Assessment of Rooftop Solar Power Technical Potential in Hanoi City, Vietnam. J. Build. Eng, 32, 101528.

[23] https://www.epa.gov/ (Accessed: 05 May 2021).